*Annals of Biomedical Engineering*, Vol. 16, pp. 463-481, 1988
Printed in the USA. 

0090-6964/88 $3.00 + .00


# COMPARISON OF NEURAL DAMAGE INDUCED BY ELECTRICAL STIMULATION WITH FARADAIC AND CAPACITOR ELECTRODES

D.B. McCreery, W.F. Agnew, T.G.H. Yuen, L.A. Bullara

Huntington Medical Research Institutes
Neurological Research Laboratory
Pasadena, California

*(Received 7/21/87; Revised 12/3/87)*

*Arrays of platinum (faradaic) and anodized, sintered tantalum pentoxide (capacitor) electrodes were implanted bilaterally in the subdural space of the parietal cortex of the cat. Two weeks after implantation both types of electrodes were pulsed for seven hours with identical waveforms consisting of controlled-current, charge-balanced, symmetric, anodic-first pulse pairs, 400 μsec/phase and a charge density of 80-100 μC/cm² (microcoulombs per square cm) at 50 pps (pulses per second). One group of animals was sacrificed immediately following stimulation and a second smaller group one week after stimulation. Tissues beneath both types of pulsed electrodes were damaged, but the difference in damage for the two electrode types was not statistically significant. Tissue beneath unpulsed electrodes was normal. At the ultrastructural level, in animals killed immediately after stimulation, shrunken and hyperchromic neurons were intermixed with neurons showing early intracellular edema. Glial cells appeared essentially normal. In animals killed one week after stimulation most of the damaged neurons had recovered, but the presence of shrunken, vacuolated and degenerating neurons showed that some of the cells were damaged irreversibly. It is concluded that most of the neural damage from stimulations of the brain surface at the level used in this study derives from processes associated with passage of the stimulus current through tissue, such as neuronal hyperactivity rather than electrochemical reactions associated with current injection across the electrode-tissue interface, since such reactions occur only with the faradaic electrodes.*

***Keywords***—*Electrical stimulation, Neural damage, Capacitor electrode.*

## INTRODUCTION

The mechanisms by which prolonged electrical stimulation induces neural damage are still largely unknown. Some studies have implicated toxic products generated at the electrode-electrolyte interface during charge injection (7,8,9,10,11). However, the

*Acknowledgments*—The authors thank Mr. Ken Kramer for fabricating the electrode arrays, Ms. Anne Hite and Louise Uffelman for technical assistance and Ms. Lorraine Kruythoff for typing the manuscript. Also, thanks to F.T. Hambrecht, M.D. for reviewing the manuscript. This work was supported by research contracts N01-NS-32359 and N01-NS-92397.

Address correspondence to D.B. McCreery, Huntington Medical Research Institutes, Neurological Research Laboratory, 734 Fairmount Avenue, Pasadena, CA 91105.

occurrence of neural damage at relatively low charge densities, using charge balanced stimulation, suggests that in many systems, other processes may contribute most of the damage (1,17,24,31).

One approach to eliminating electrochemical reactions at the electrode-tissue interface during surface stimulation of the brain is by the use of capacitor electrodes. Capacitor electrodes are fabricated by anodizing a metal surface with a thin layer of dielectric material such as tantalum pentoxide (8,12,13,14,18,25,27,28). With these electrodes the current pulses are injected across the electrode surface by capacitive charging without the oxidation-reduction (faradaic) reactions which occur with noble metal electrodes.

This study was designed to utilize these differences in noble metal and capacitor electrodes to provide insights into the mechanisms of neural damage due to electrical stimulation of the brain surface (2,3,22,23,30). Neural damage beneath capacitor electrodes can be attributed only to mechanical factors related to the presence of the electrode or to factors associated with the passage of current through the tissue, whereas neurons beneath pulsed platinum electrodes could be damaged by electrochemical reactions (including the products of electrode dissolution) as well.

## METHODS

### *Electrodes and Stimulation Protocols*

The faradaic electrodes were platinum discs, 1.1 mm in diameter. The capacitor (nonfaradaic) electrodes were sintered pellet, anodized tantalum-tantalum pentoxide units, 1.0 mm in diameter, supplied by Sprague, Inc. The platinum electrodes were embedded in silicone elastomer (Dow-Corning, Type A Medical Grade Adhesive) leaving exposed only the lower surface of each disc. The capacitor electrodes were mounted in recesses in the silicone 1.1 mm in diameter; the small gap around the sides permits better utilization of the capacitance. Thus, when implanted in the subdural space, both types of electrodes will face the pia through round windows with an area of 0.01 $cm^2$ and thus, the current density in the subjacent brain tissue should be the same when the identical current waveform is injected through both electrode types. The capacitance of the tantalum electrodes ranged from 0.15–0.25 $\mu$F as determined by low frequency potentiodynamic cycling (1 v/sec), and with the mounting described above, the utilizable capacitance (I/(dv/dt)), during injection of the 400 $\mu$sec controlled-current pulses was 0.05–0.07 $\mu$F. The embedded discs were mounted on porous polyester matrices molded to conform to the shape of the cat's gyrus suprasylvius. The capacitor electrodes, as well as the associated ancillary structures (leads, junctions, etc.) were tested for electrical integrity by soaking for 24 hours in 0.9% NaCl solution with +27 volts dc between the leads and a carbon counterelectrode. The electrode assemblies were tested for dc leakage current at four volts positive to the potential of hydrogen evolution. Assemblies whose leakage exceeded 0.05 $\mu$A were rejected.

The arrays were then cleaned by mild sonication in ethanol and distilled water and sterilized with ethylene oxide. At least 24 hours after sterilization, two arrays containing a platinum and a capacitor electrode (four discs) were implanted bilaterally in the subdural space over the parietal (gyrus suprasylvius) cortex of 25 adult or adolescent cats of either sex (Fig. 1). A total of 100 electrodes of both types was implanted. A large (1 $cm^2$) platinum counterelectrode was implanted beneath the

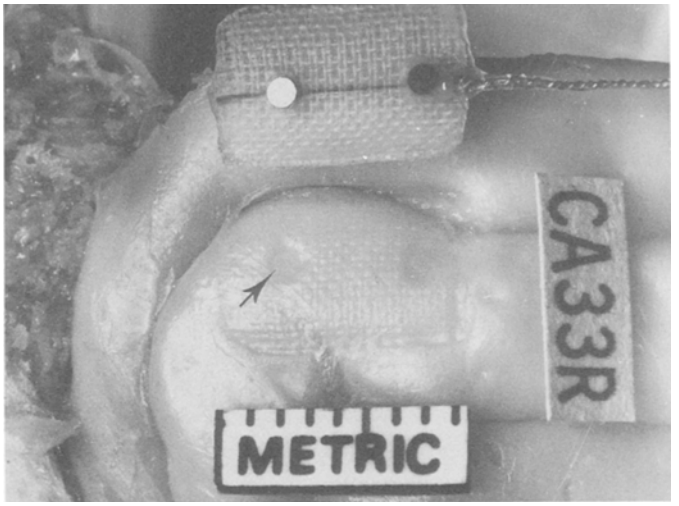


**FIGURE 1. Autopsy view of the 2 electrode sites on the right gyrus suprasylvius. The posterior (platinum) electrode site (arrow) is clearly visible while the anterior (tantalum pentoxide) electrode site is visible, but poorly defined due to the presence of an annulus of tissue surrounding the electrode (note tissue surrounding the dark tantalum penotxide electrode). In this instance the platinum electrode was free of this annulus but in other cases a tissue distribution similar to that seen around the tantalum pentoxide electrodes was present.**

temporal muscle adjacent to one of the craniectomy defects. The procedure was performed using general anesthesia (nitrous oxide and halothane) and aseptic surgical technique.

Two weeks after implantation and just prior to pulsing, the cats were anesthetized with pentobarbital and the implanted capacitor electrodes were tested for dc leakage at +4 and +20 volts with respect to the implanted platinum counterelectrode. Electrodes with zero or slight dc leakage were pulsed if the leakage current was less than 10 $\mu$A at +20 volts with respect to the counterelectrode. However, the histological data were considered only if, upon dc bubble testing of the (recovered) array, the site of any leakage could be shown to be remote (at least 2 mm) from the electrode pellet.

The platinum and capacitor electrodes were pulsed against the large counterelectrodes with identical waveforms (controlled current, charge-balanced, symmetric, anodic-first pulse pairs, 400 $\mu$sec/ph in duration with no delay between the anodic and cathodic phases). Between pulse pairs, the potential of the platinum stimulating electrodes was returned to that of the platinum counterelectrode through a large (500 kOhms) resistance. Since the capacitor and platinum electrodes were both embedded in silicone and faced the pia through circular windows of essentially the same diameters and areas, the identical current waveform was used with both types of electrodes to ensure a similar time course of current density in the subjacent brain. In addition, to ensure precise charge balance over time, all electrodes were coupled to the stimulus current source through 4.7 $\mu$F Mylar capacitors. This stimulus waveform is nearly ideal for pulsing faradaic electrodes, providing optimal (although not neces-

sarily complete) reversal of electrochemical charge injection processes at the metal-electrolyte interface (9,10,11). It has been used in previous studies of platinum stimulating electrodes conducted in our laboratory (2,3,4,17,24,31); however, this biphasic waveform is by no means ideal for capacitor electrodes. Because of the semiconductor nature of the tantalum oxide, such electrodes must be pulsed anodic first, but if the anodic charge is subsequently removed quickly, as occurs with a symmetrical pulse pair, the electrode potential overshoots the interpulse baseline (sometimes by several volts). The negative overshoot may be sufficient to cause the tantalum oxide to conduct, causing the capacitor electrode to behave momentarily as a faradaic electrode. This conduction can be observed as a decrease in the slope near the end of the cathodic phase of the voltage transient induced across the electrode by the stimulus current pulse. The negative-going overshoot is probably due to the multiple time constants which arise from part of the capacitance being in series with the relatively large ohmic resistance of the pores in the electrode pellet (12). During injection of short, high amplitude current pulses, these longer time constants charge and discharge more slowly than does the capacitance near the geometric surface of the electrode, thereby producing the overshoot of the interpulse voltage during the charge removal process. Therefore, the interpulse (baseline) potential of the capacitor electrode was biased up to 4 volts positive of the platinum counterelectrode, placing the interpulse potential further from the point at which the oxide begins to conduct. For each electrode, the pulse amplitude was set and the bias was increased until additional bias produced no further decrease in the slope at the end of the cathodic phase of the voltage transient. The same bias was placed on the second capacitor electrode, if it passed the prestimulus dc leakage test. The bias produced no measureable effect on the current pulse pairs.

In all animals, the transient and interpulse potential was monitored on an oscilloscope against the platinum counterelectrode. Also, in eight animals, the (biased) interpulse potential was monitored during pulsing by means of a chronically implanted Ag/AgCl reference electrode coated with methyl methacrylate and embedded in the muscle adjacent to the craniectomy defect. This reference electrode carries no current, providing a crude 3-electrode system. The potential of the implanted Ag/AgCl electrode was in turn measured several times during the experiment against a saturated calomel electrode (SCE) placed in the cat's mouth. By this means, the current-carrying platinum counterelectrode was seen to polarize somewhat (up to $-200$ mv SCE) at the start of pulsing, but then to maintain that potential (within $\pm$ 30 mV) throughout the 7 hours of stimulation.

At least one capacitor electrode and one faradaic (platinum) electrode were pulsed continuously, for 7 hours at 50 pps. The animals remained under light pentobarbital anesthesia throughout the stimulation. In all but one animal, the same pulse amplitude was used with the capacitor and platinum electrodes. In each animal the highest current, up to 2.5 mA, which did not drive a capacitor electrode beyond the capacitor dielectric formation voltage (+ 30 volts vs. the saturated calomel electrode) was used. This ranged from 0.8 to 1 $\mu$C/ph. The corresponding charge densities, based on the electrode's "geometric" surface areas, ranged from 80 to 100 $\mu$C/$cm^2 \cdot$ph. After the seven hours of stimulation the capacitor electrodes were again tested for dc leakage as described above.

Recording of compound action potentials (CAPs) from the pyramidal tract was omitted in the animals in the present study in which electrodes had been chronically

implanted, since the physiologic effectiveness of stimulation of the motor cortex at the range of the pulse amplitudes used was demonstrated previously (17). However, an acute experiment, also using pentobarbital anesthesia was performed, in which the CAP was recorded from the ipsilateral pyramidal tract via a monopolar electrode (16) while the same spot on the precruciate cortex was stimulated at 50 pps, first with a platinum electrode (mounted in its array), then with a mounted capacitor electrode.

### *Histologic Methods*

Eighteen animals were killed within 20–30 minutes following termination of seven hours of stimulation. Two were killed one week after stimulation. Aortic perfusion was carried out under general anesthesia. For light microscopy, a prewash of approximately 1 liter of 0.9% NaCl was perfused at a gravity flow pressure of 120 mm Hg. This was followed by perfusion of 2 liters of unbuffered 10% formalin at the same pressure. In three animals used for electron microscopy, the prewash was followed by 2 liters of one-half strength Karnovsky's solution (2.5% glutaraldehyde, 2.0% paraformaldehyde in 0.1 M sodium cacodylate buffer). Continued fixation of the brain was carried out by placing the head in the respective fixatives until autopsy the following day.

At autopsy, bone flaps and dura were removed to reveal the array on each gyrus suprasylvius. Photographs were taken of the array sites before and after removal of the array.

Parasagittal blocks of tissue were cut to include both electrode sites in each hemisphere, in addition to a remote control block from the frontal cortex. The tissue sites were marked by horizontal punch holes, made with a no. 20 needle, below each electrode site. In addition, the boundaries of the disc sites were marked by inserting needles tipped with India ink. For light microscopy, the blocks were further fixed, dehydrated and embedded in paraffin. Parasagittal sections six $\mu$m in thickness were made to include both electrode sites on each hemisphere. Serial sections were alternately stained with Nissl, H&E and Masson's trichrome.

For electron microscopy 1 $mm^3$ blocks were post-fixed in 2.0% osmium tetroxide in 0.1 molar sodium cacodylate buffer. Following graded alcohol dehydration the tissues were embedded in Polysciences Polybed 812 resin. Plastic sections 1 $\mu$m thick were stained with Richardson's-toluidine blue (2:1). Ultrathin sections were stained with uranyl acetate and lead citrate.

## RESULTS

Figure 2 shows CAPs recorded from the ipsilateral pyramidal tract, evoked by a capacitor and a platinum electrode, pulsed at 2.0 mA and 50 pps. The directly-evoked (early) and transsynaptically evoked (late) components of the CAPs are nearly identical for the two electrode types. Since shifting the position of the stimulating electrode by only a small fraction of its diameter produced a large change in the amplitude of the CAPs (especially in the late components) the similarity of the two CAPs indicates that the two electrodes evoked neuronal activity with similar efficiency.

At autopsy, the dura overlying the electrode array was usually slightly thickened. In most cases, the dura was easily reflected from the external capsule of connective tissue overlying the arrays. The layer of connective tissue between the electrodes and the pia was usually thin, although in two animals a thicker layer of tissue (approxi-

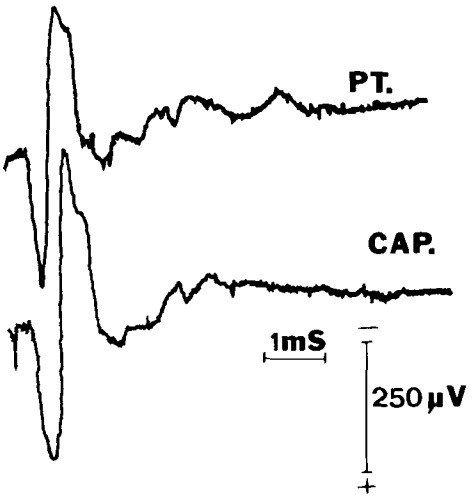


**FIGURE 2. Compound action potentials recorded from the ipsilateral pyramidal tract during stimulation of the precruciate gyrus with a platinum electrode, and a capacitor electrode. Each record is the average of 10 consecutive evoked responses.**

mately 0.5 mm to 0.7 mm in thickness) was observed. Data from these sites were excluded from the series, since it is likely the stimulus current can disperse in such a pad of tissue, effectively reducing the current density (and charge density) at the pia. Also, any toxic products formed at the electrode interface can disperse in such a pad. The contour of the polyester mesh matrix, which was curved to fit the gyrus, appeared intact. After removal of the array, the imprint of the matrix and the electrode discs often were visible on the surface of the brain (Fig. 1). In a few instances, an annulus of firmly attached connective tissue had formed around the discs. In addition to the 4 sites lost to formation of connective tissue, electrode sites in which the electrode had migrated to lie atop a sulcus also were excluded (four sites), as were those capacitor electrodes which did not meet the dc current leakage criteria described above after the end of the seven hours of stimulation. (Capacitor electrodes which did not meet the leakage criteria before the start of the stimulation were used as unpulsed controls.) In two animals, the electrodes became shorted together during the ten days before pulsing, due to intrusion of fluid into the cable or transcutaneous connector. Also, animals in which at least one pulsed capacitor electrode was not acceptable after the poststimulation leakage test were not perfused. This left 65 of the original 100 electrodes from 20 of the 25 animals of which 54 were examined. The tissue beneath 11 of the unpulsed platinum electrodes were not examined, as discussed below.

### *Histologic Findings*

Fifty electrode sites were examined at the light microscope level only, and eight additional sites from three cats were examined at both the light and the transmission electron microscope level. One of the cats perfused for electron microscopy had been killed immediately after the end of stimulation and two others were killed one week later. Tissue collected from sites on the frontal lobe, remote from the electrode

arrays, showed normal leptomeninges and molecular layer. The underlying neurons also appeared normal.

Table 1 summarizes the histologic findings at the light microscope level for brain tissue subjacent to 16 pulsed capacitor electrodes and 17 pulsed platinum electrodes from the 18 animals killed immediately after the end of stimulation. Six of the platinum sites were stimulated at 0.8 $\mu$C/ph, five at 0.88 $\mu$C/ph and six at 1 $\mu$C/ph. Four of the capacitor sites were stimulated at 0.8 $\mu$C/ph, six at 0.88 $\mu$C/ph and seven at 1 $\mu$C/ph. Fourteen unpulsed capacitor sites and three unpulsed platinum sites also were examined. Of the 22 sites from these 18 animals not enumerated in Table 1, six capacitor sites were lost, either because the electrode developed large leakage currents during pulsing, or they were found at autopsy to lie atop a sulcus. Five of the pulsed platinum sites also were lost. Eleven of the unpulsed platinum electrodes were not prepared and examined due to our familiarity with the biocompatability of unpulsed platinum from previous studies (3,4,23,24).

Tissue beneath all of the unpulsed platinum electrodes and most of the unpulsed capacitor electrodes appeared normal (Fig. 3). Tissue beneath the edges of two of the unpulsed capacitor electrodes contained foci of minimal (grade 1) damage, probably due to mechanical compression of the cortex by the rather sharp edges of the slightly protruding discs. The leptomeninges beneath most of the unpulsed electrodes

**TABLE 1.**

| Electrode Material | Pulsed/ Unpulsed | Total Sites | Severity of neural damage | | | | |
|---|---|---|---|---|---|---|---|
| | | | 0 | + | ++ | +++ | ++++ |
| Platinum | Unpulsed | 3 | 3 | 0 | 0 | 0 | 0 |
| Platinum | Pulsed | 17 | 1 | 1 | 1 | 1 | 13 |
| Capacitor | Unpulsed | 14 | 12 | 2 | 0 | 0 | 0 |
| Capacitor | Pulsed | 16 | 1 | 2 | 1 | 4 | 8 |

Data are from 18 animals killed after 7 hours of stimulation. Twenty-two of 72 electrode sites are not included. Only 3 unpulsed platinum sites were examined due to abundant extant data attesting to biocompatibility of subdural implants of this metal (see text, Results section).

Stimulus parameters: Charge/phase was 0.8–1.0 $\mu$C/ph using 2.0–2.5 mA pulse duration of 400 $\mu$sec and a frequency of 50 pps for 7 hours. Charge densities ranged from 80–100 $\mu C/cm^2 \cdot ph$, (see Methods Section for further details on parameters).

Damage code:

| | | |
|---|---|---|
| + | minimal | Slight neuronal shrinkage with or without hyperchromism or a small number of neurons undergoing degeneration. |
| ++ | mild | Increased neuronal shrinkage approaching a stellate profile. Thin pericellular halo, or a few neurons undergoing degeneration. |
| +++ | moderate | Moderately shrunken, stellate, hyperchromic neurons. Widened perineuronal halo, or a moderate number of neurons undergoing degeneration. |
| ++++ | severe | Markedly shrunken, stellate, hyperchromic neurons with large perineuronal halos. Damage extending through most or all layers with or without neuronal loss. |

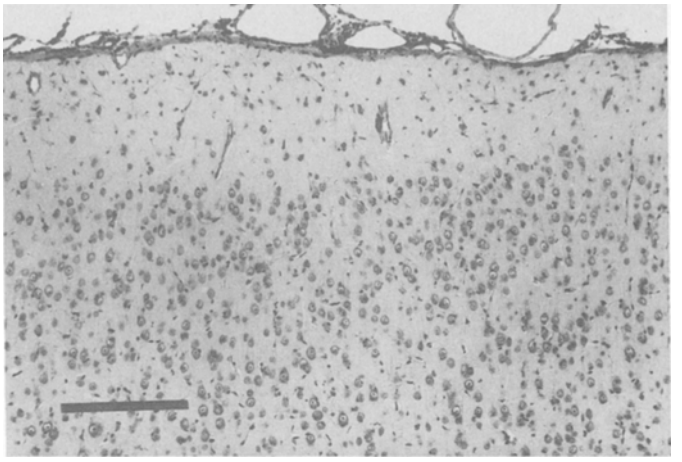

**FIGURE 3. Parietal cortex beneath unpulsed tantalum electrode. The leptomeninges are not appreciably thickened and the molecular and neuronal layers appear indistinguishable from control cortex remote from any array. Nissl stain. Bar = 300 $\mu$m.**

was usually somewhat thickened and there was often slight gliosis of the underlying molecular layer.

Neural damage at sites immediately subjacent to pulsed platinum or capacitor electrodes in animals killed immediately after seven hours of stimulation was qualitatively the same although the severity of the damage was on the average slightly less beneath the capacitor electrodes. However, this difference was not significant in a 2-sided chi-square test of homogeneity ($\chi^2 = 1.46$, $df = 4$, $p = 0.4$). There was also only a very small positive correlation between the severity of the damage and the intensity of the stimulation over the small range used (0.8–1 $\mu$C/ph). The slopes of the regression lines were 0.71 damage grades/$\mu$C for the platinum electrodes, and 0.75 grades/$\mu$C for the capacitors. However, there was considerable variability, and damage ranged from grade 0 or 1, to 4 at both 0.8 and 1 $\mu$C/ph for both electrode types. The damage beneath electrodes with a small amount of dc leakage current was not greater than beneath those exhibiting no detectable leakage. When moderate leakage (less than 10 $\mu$A at 20 volts) occurred, the location of the leak was found to be at a site remote from the actual electrode pellet and did not effect the tissue immediately subjacent to the pellet.

The damage beneath the pulsed electrodes consisted primarily of stellate profiles of shrunken hyperchromic neurons usually extending to a depth of no more than 750 $\mu$m but often extending across the full diameter of the electrode discs. The leptomeninges were somewhat thickened and infiltrated by large and small mononuclear cells and eosinophils sometimes accompanied by perivascular cuffing. In severely damaged tissue the neurons were more severely shrunken and hyperchromic, and the perineuronal halos were more pronounced (Figs. 4 and 5).

At the electron microscopy level, tissue beneath unpulsed electrodes appeared normal (Fig. 6); whereas the ultrastructure of three pulsed electrode sites pulsed at 1 $\mu$C/ph (1 platinum and 2 capacitors) from the animal killed immediately after stim-

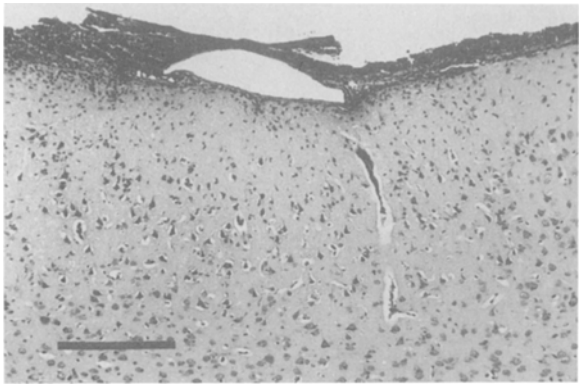

**FIGURE 4. Platinum electrode site pulsed with 88 $\mu C/cm^2 \cdot ph$ and a charge per phase of 0.88 $\mu C/ph$ for 7 hr. The leptomeninges are infiltrated and overlaid by numerous mononuclear cells and neutrophils (confirmed by observation at greater magnification). The latter have permeated the molecular and upper neuronal layers. Gliosis is not present. The uppermost neurons are markedly shrunken, hyperchromic and surrounded by wide perineuronal haloes. Nissl stain. Bar = 300 $\mu$m.**

ulation, all showed a gradation of neuronal damage ranging from damaged mitochondria with loss of cristae, (Figs. 7 and 8) intracellular edema (Figs. 9–11) to shrunken, hyperchromic "dark neurons" (Figs. 12–14). Degenerative stages of neurons were accompanied by vigorous phagocytic activity by both neutrophils and macrophages (Fig. 15). Other cell types, including endothelial, astrocytes and oligodendrocytes often immediately adjacent to damaged neurons, appeared normal (Fig. 12).

At one week poststimulation, four electrode sites pulsed at 1 $\mu C/ph$ (2 capacitor and 2 platinum electrodes) showed less damage than immediately after stimulation, particularly when studied by the light microscope. At the ultrastructural level, how-

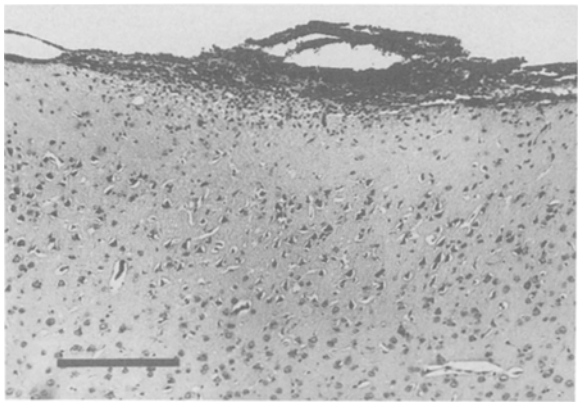

**FIGURE 5. Tantalum pentoxide electrode site pulsed with 88 $\mu C/cm^2 \cdot ph$. The findings are essentially the same as those in Fig. 3. Nissl stain. Bar = 300 $\mu$m.**

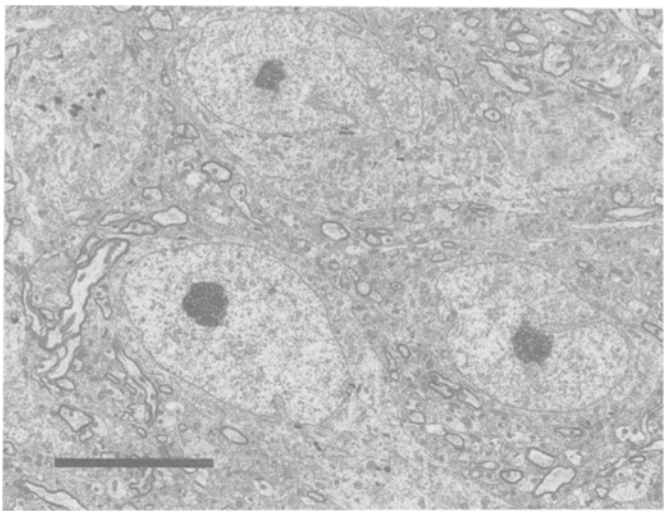

**FIGURE 6. Electron micrograph beneath unpulsed Pt electrode. Five neurons and surrounding neuropil appear normal. Bar = 10 $\mu$m.**

ever, markedly shrunken, often fragmented dark cell profiles and degenerating axons were frequently observed indicating irreversible damage to some neurons. Degenerating cellular elements were usually accompanied by macrophages engaged in scavenging damaged cell remnants (Figs. 16 and 17).

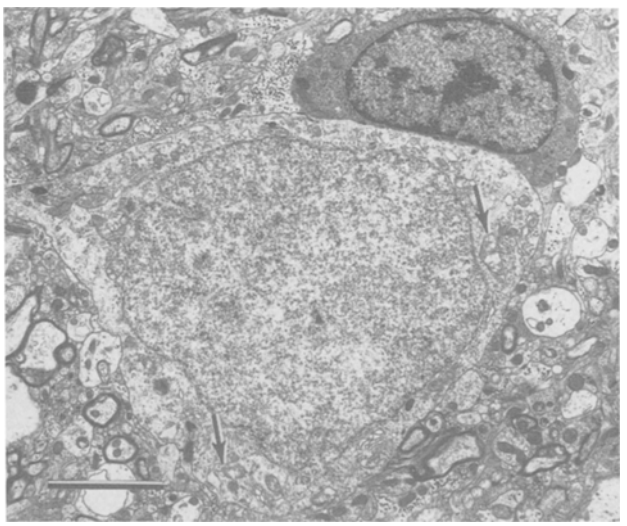

**FIGURE 7. Early neuronal damage characterized by peripheral cytoplasmic edema and swelling with rarefaction of mitochondria (arrows). The adjacent oligodendrocyte does not show such changes. Bar = 4 $\mu$m.**

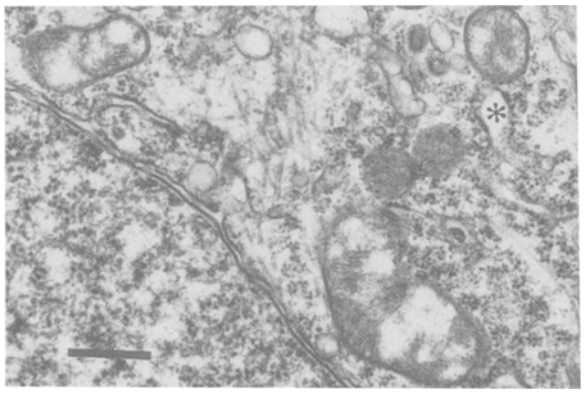

**FIGURE 8. Greater magnification of mitochondria in Fig. 7, showing marked rarefaction and loss of cristae, and dilatation of rough endoplasmic reticulum (asterisk). Bar = 0.5 $\mu$m.**

## DISCUSSION

These results demonstrate that charge-balanced pulse pairs of 0.8–1.0 $\mu$C per phase and a charge density of 80–100 $\mu C/cm^2$ applied at the brain surface for seven hours, at a frequency of 50 pulses per second, induces a comparable amount of neural damage, whether delivered through platinum or tantalum pentoxide disc electrodes. The damage beneath most (25) of the pulsed platinum and capacitor electrodes from animals killed immediately after stimulation was moderate to severe and at least partially irreversible. Five pulsed electrodes (3 capacitor and 2 platinum) induced only mild

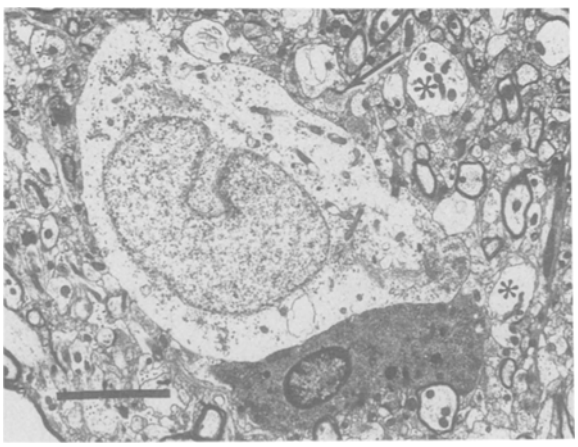

**FIGURE 9. Neuron (center) showing swollen mitochondria with loss of cristae and generalized cytoplasmic edema. Aside from a single swollen mitochondrion, the subjacent oligodendrocyte appears normal. The surrounding neuropil contains several edematous cell profiles, presumably dendrites (asterisks). Note the lack of extracellular edema. Bar = 10 $\mu$m.**

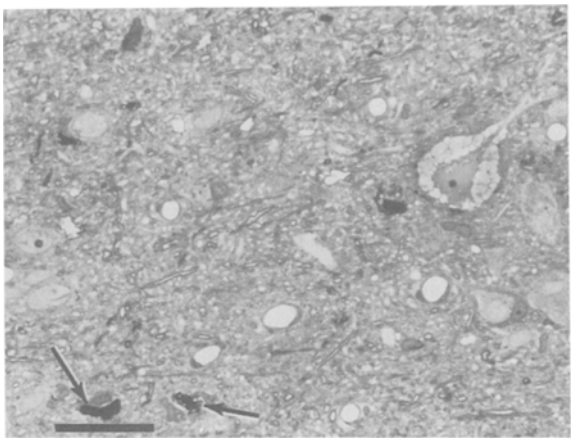

**FIGURE 10. Upper neuronal layers showing several presumptive neurons in a state of marked shrinkage and hyperchromism (arrows). One neuron (right center) shows an earlier stage of damage, with severe peripheral vacuolation (compare with Fig. 10). Bar = 40 μm.**

or minimal neural damage. The cause of such variability in the severity of the damage is unknown, but it may be related to the thickness of the layer of connective tissue which often develops between the implanted array and the pia. Although data from animals in which the connective tissue was greatly thickened were excluded (greater than approximately 0.5 mm or half the diameter of the stimulating electrodes), the variability in the thickness of even the thinner layers would be expected to cause some variability between animals in the dispersion of stimulus current above the pia. When minimum connective tissue was present and the pulsed electrodes left

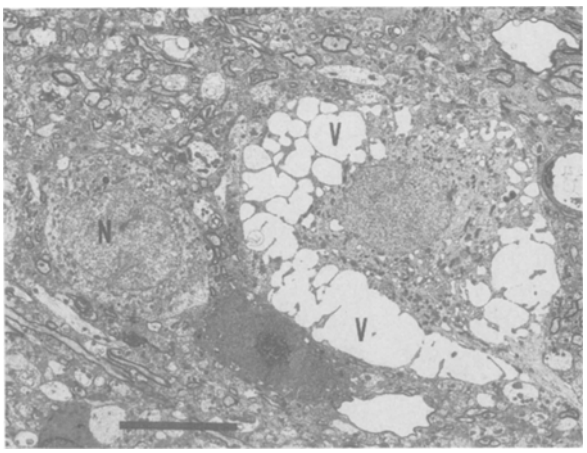


**FIGURE 11. Two neurons showing marked differences in damage. The more intact neuron (N) contains only a few swollen mitochondria and appears relatively normal while the adjacent neuron contains marked cytoplasmic vacuolations (V). Bar = 10 μm.**

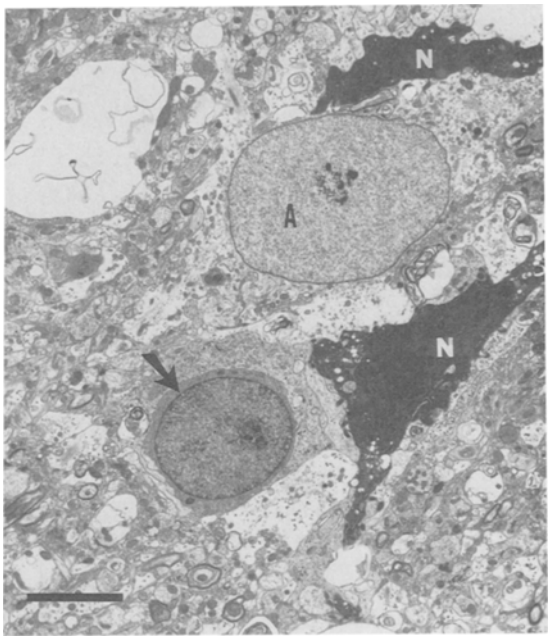


**FIGURE 12. Two markedly damaged and shrunken neurons accompanied by a relatively normal-appearing oligodendrocyte (arrow) and astrocyte (A). This hierarchy of cellular vulnerability to damage was a constant finding. Bar = 5 $\mu$m.**

distinct impressions on the pia of the fixed brain (e.g., Fig. 1), then damage to the subjacent neurons was always moderate to severe. Conversely, in those animals in which connective tissue had developed into conspicuous "pads" greater than approximately 0.5 mm in thickness, the neurons beneath pulsed platinum and tantalum electrodes were undamaged, possibly because the current at the actual surface of its brain was more dispersed.

Our results are not in agreement with those of Bernstein *et al.* (8), who tested similar anodized, sintered pellet tantalum electrodes implanted chronically on the cat's cerebral cortex. These authors reported no damage subjacent to the pulsed electrodes. However, they did describe thick pads of connective tissue adherent to the tantalum discs, and their experimental design did not include pulsing faradaic electrodes and looking for neural damage beneath these, which would have served as a control for the experimental conditions, including dispersion of stimulus current by such interposed connective tissues.

Auer *et al.* (5,6), in an ultrastructural study of hypoglycemic brain damage, demonstrated that neither "dark" (hyperchromic) neuronal change or extensive mitochondrial alterations can be considered hallmarks of lethally injured neurons. He noted ultrastructural indicators of fatal cellular injury as "amorphous cytoplasm lacking ribosomes and Golgi apparatus, mitochondria containing flocculent densities, thick, electron dense chromatin clumps, large breaks in the nuclear and cell membranes, rupture of cytoplasmic contents into the extracellular space (cytorrhexis) and herniation of nuclear contents into the cytoplasma (karyorrhexis)." In the present study

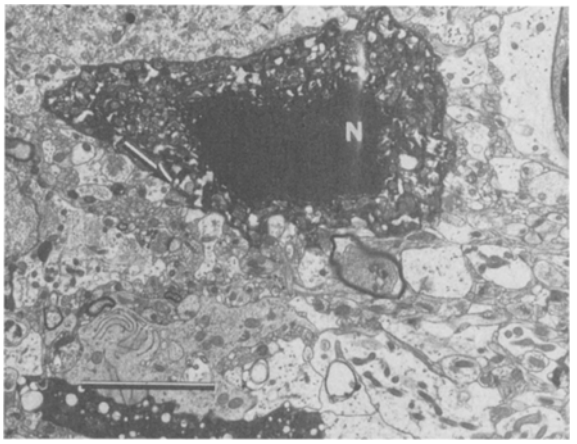


**FIGURE 13. Portions of two markedly shrunken, hyperchromic neurons (center and bottom of micrograph). Many cell profiles in the adjacent neuropil appear rarefied and edematous. The axosomatic synapse (arrow, and see Fig. 13) confirms the neuronal nature of the damaged cell. Bar = 5 μm. ×5,500.**

these changes, as well as later stages (cytolysis and phagocytosis by macrophages and neutrophils) were observed in some neurons. Although morphometric analyses were not carried out, it was apparent from comparing the data from animals killed immediately and one week after stimulation, that most of the neurons undergoing shrinkage immediately after stimulation had recovered. There were fewer profiles of degenerating neurons one week after stimulation (compared to immediately after stimulation) and a similar neuronal density, as assessed by either light or electron

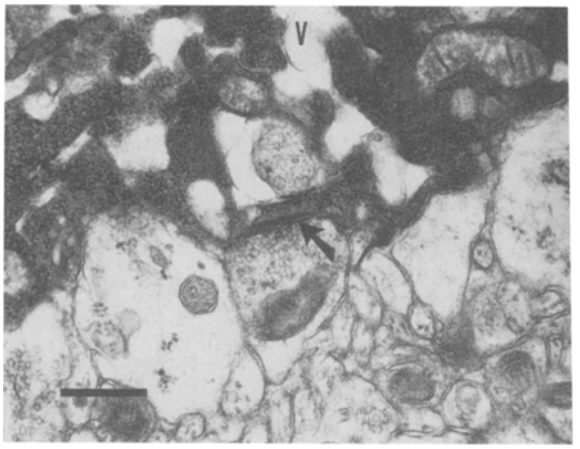


**FIGURE 14. Axosomatic synapse (arrow) shown in Fig. 12. Note the severe vacuolation (V) in the neuronal cytoplasm and the marked cytoplasmic attenuation. Bar = 0.5 μm.**

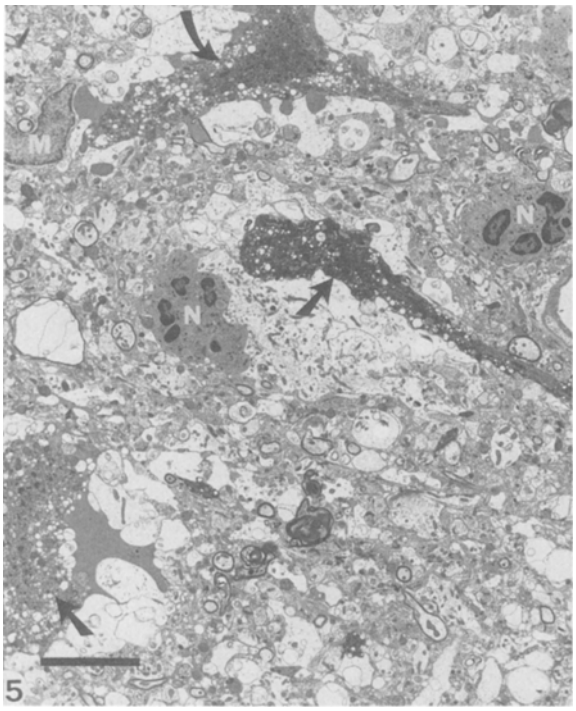


**FIGURE 15. Three degenerating neurons (arrows) and adjacent edematous neuropil (numerous pale cellular profiles). Phagocytosis of damaged cells is indicated by the presence of a macrophage (M) and 2 extravascular neutrophils (N). Bar = 10 $\mu$m.**

microscopy. However, the widespread phagocytic activity (removal of the necrotic cells) after one week firmly establishes that some of the cells were irreversibly damaged. The obscuring of organelles by the extreme cytoplasic density of the degenerating profiles made identification difficult. However, these cells were positively identified as neurons by the presence of axosomatic synaptic processes.

At the stimulus charge density used in the present study (80–100 $\mu C/cm^2 \cdot ph$) grade 5 damage, with necrosis and loss of tissue architecture was not seen (Table 1). However, such damage has been elicited with higher charge densities and more prolonged stimulations (3,4). In the present study, the ultrastructural pattern of damage was that of a selective vulnerability of neurons over glial cells. Fibrous astrocytes in the molecular layer were consistently spared, whereas neurons 100 to 200 $\mu$m from the pia were most frequently damaged. In many fields, oligodendrocytes and astrocytes were observed immediately adjacent to neurons and dendrites in various stages of degeneration. This highly selective damage suggests factors associated with neuronal hyperactivity and/or extreme electrical hyperpolarization/depolarization of neurons as the causative mechanism.

Other insults to the brain known to produce dark and irreversibly damaged neurons include hypoglycemia, the chemical convulsants kainic acid (29), folic acid (20) and sustained electrical stimulation of the perforant pathway (19). In the latter study,

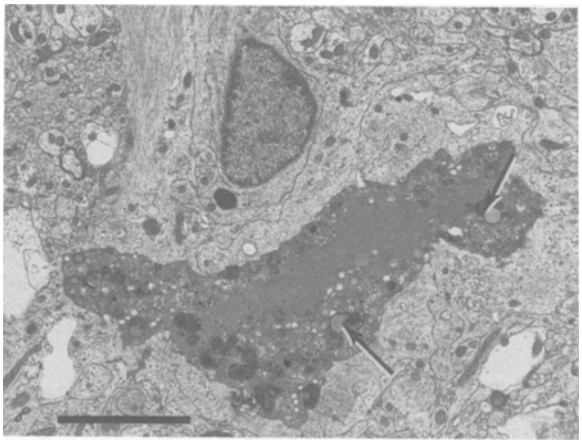

**FIGURE 16. Pulsed Ta-$Ta_2O_5$ electrode site fixed 1 wk. after stimulation. The degenerating cell is presumably a neuron inasmuch as the cytoplasm contains lipofuscin (arrows) and other cell types (astrocytes and oligodendroglia) were never seen degenerating. A macrophage is present above the damaged neuron. Bar = 4 $\mu$m.**

the affected hippocampal neurons were activated indirectly via the stimulated afferent tract so the neural damage was ascribed to prolonged neuronal hyperactivity. These authors observed hyperchromic, shrunken neurons intermixed with those with marked intracellular edema. This is similar to the ultrastructural findings in the hippocampus following systemic administration of exogenous excitotoxins (e.g., kainic acid), or following induction of status epilepticus by other means, and also the findings from the present study after several hours of continuous stimulation. Some

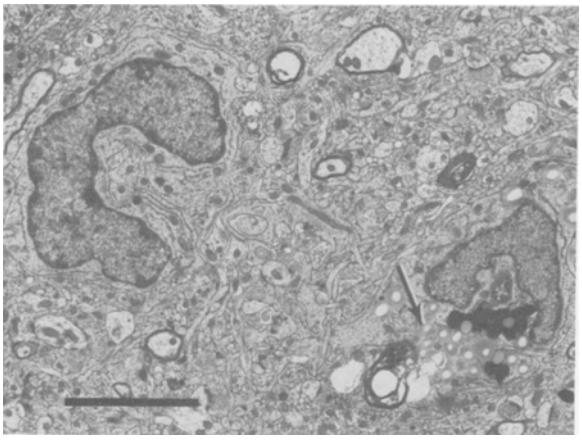

**FIGURE 17. Same electrode site as that shown in Fig. 16. One of 2 macrophages contains cellular debris and lipid inclusions (arrows). Aside from an occasional deranged axon, the surrounding neuropil appears normal. Bar = 5 $\mu$m.**

workers (16,19,20) have hypothesized that intracellular edema is the early stage of the damage sequela and in fact is the primary damaging factor (16,19). While our histopathologic findings are very similar to theirs, identification of the specific metabolic mechanism responsible for this pattern of damage must await biochemical investigations.

It is unlikely that hypoxia, either from vasogenic factors (oligemia) or from increased $0_2$ consumption during hyperactivity contributes significantly to the neural damage. In the present study, the extracellular edema which occurs early in hypoxic brain damage (21) was not observed. Other studies have shown that increased blood flow adequately compensates for the increased oxygen demand in the hippocampus during neuronal hyperactivity accompanying kainate seizures (22). Also, Bartlett *et al.* (7) were not able to reduce neural damage in the cortex during electrical stimulation by dilating central blood vessels with $CO_2$.

A number of possibly hazardous charge transfer reactions have been demonstrated or hypothesized to occur at the surface of a platinum stimulating electrode. Brummer & Turner (10) suggested that evolution of hydrogen or oxygen may be hazardous in part because of the pH changes which may accompany the resulting imbalance of injected charge. This is due to the partial electrochemical irreversibility of the gas evolution reactions. However, these authors calculated the nongassing charge capacity of platinum electrodes to be 350 $\mu C/cm^2$ for anodic-first pulses (9), which is greater than the maximum charge density used in our experiments. However, other possibly hazardous reactions may occur at lower charge densities including dissolution of the metal electrode (8,26), or reduction of oxygen to peroxide (15). The present study indicates that these and other electrochemical processes contribute, at most, a minor component to the neural damage induced by surface electrodes pulsed with charge-balanced pulses, even at the moderately high charge densities of 80–100 $\mu C/cm^2$ geometric, since they can occur only with the platinum electrodes and both types of electrodes induced similar damage. Thus, even at these rather high charge densities, most of the neural damage seems to be due to passage of the stimulus current through the tissue, rather than the processes by which the current is injected across the metal-electrolyte interface. The former category would include, but would not be limited to, the evoked neuronal hyperactivity (19).

Finally, the stimulus waveform used in this study is nearly ideal for faradaic electrodes (symmetrical, actively charge-balanced pulse pairs). With electrode materials more subject to corrosion than is platinum, with higher charge densities, or with stimulus waveforms which permit injection of significant net charge (e.g., monophasic, direct-coupled pulses), it is likely that faradaic reactions could contribute more substantially to the neural damage.

These findings have several important connotations. First, they provide insight into the mechanisms of neural damage induced by stimulation of the brain which have practical implications with regard to functional electrical stimulation. They also indicate that direct contact between the electrode and nervous tissue is not essential for the production of neural damage. Thus, it is possible that neural damage may be induced by prolonged use of the high intensity extracranial stimuli employed for evoked potential studies during various neurologic procedures (1,30).

*Abbreviations*—$\mu C$ = microcoulomb, ph = phase, $\mu F$ = microfarad, CAP = compound action potential, pps = pulses (stimulations) per second.

## REFERENCES


1. Agnew, W.F.; McCreery, D.B. Considerations for safety in the use of extracranial stimulation for motor evoked potentials. Neurosurg. 20:143–147; 1987.
2. Agnew, W.F.; Yuen, T.G.H.; McCreery, D.B. Morphologic changes after prolonged electrical stimulation of the cat's cortex at defined charge densities. Exp. Neurol. 79:397–411; 1983.
3. Agnew, W.F.; Yuen, T.G.H.; Bullara, L.A.; Jacques, D.; Pudenz, R.H. Intracellular calcium deposition in brain following electrical stimulation. Neurol. Res. 1:187–202; 1979.
4. Agnew, W.F.; Yuen, T.G.H.; Pudenz, R.H.; Bullara, L.A. Electrical stimulation of the brain: IV. Ultrastructural studies. Surg. Neurol. 4:438–448; 1975.
5. Auer, R.N. Hypoglycemic brain damage. Doctoral Thesis, University of Lund; 1985.
6. Auer, R.N.; Wieloch, T.; Olsson, Y.; Siesjo, B.K. The distribution of hypoglycemic brain damage. Acta. Neuropath. 64:177–191; 1984.
7. Bartlett, J.R.; Doty, R.W.; Lee, B.B.; Negrao, N.; Overman, W.H. Deleterious effects of prolonged electrical excitation of striate cortex in Macaques. Brain Behav. & Evol. 14:46–66; 1977.
8. Bernstein, J.J.; Hench, L.L.; Johnson, P.F.; Dawson, W.W.; Hunter, G. Electrical stimulation of the cortex with tantalum pentoxide capacitor electrodes. In: Hambrect, F.T.; Reswick, J.B., eds. Functional Electrical Stimulation. New York: Marcel Dekker, Inc.; Basel 1977.
9. Brummer, S.B.; Turner, M.J. Electrical stimulation with Pt electrodes; analysis of dissolved platinum and other dissolved electrochemical products. Brain, Behav. & Evol. 14:23–45; 1977.
10. Brummer, S.B.; Turner, M.J. Electrical stimulation with Pt electrodes. II. Estimation of maximum surface redox (theoretical non-gassing) limits. IEEE Trans. Biomed. Engr. BME-24: 440–443; 1977a.
11. Brummer, S.B.; Turner, M.J. Electrochemical considerations for safe electrical stimulation of the nervous system with platinum electrodes. IEEE Trans. Biomed. Eng. 24:59–63; 1977b.
12. Guyton, D.L.; Hambrecht, F.T. Theory and design of capacitor electrodes for chronic stimulation. Med. Biol. Engr. 12:613–620; 1974.
13. Guyton, D.L.; Hambrecht, F.T. Capacitor electrodes stimulate nerve or muscle without oxidation-reduction reactions. Science (United States) 6. 181:74–76; 1973.
14. Johnson, P.F.; Bernstein, J.J.; Hunter, G.; Dawson, W.W.; Hench, L.L. An *in vitro* and *in vivo* analysis of anodized tantalum capacitive electrodes: Corrosion response, physiology, and histology. J. Biomed. Mater. Res. 11:637–656; 1977.
15. Lamb, B.S.; Webb, R.C. Vascular effects of free radicals generated by electrical stimulation. Am. J. Physiol. 247:709–714; 1984.
16. Lassman, H.; Petsche, U.; Kitz, K.; Baran, H.; Sperl, G.; Settelberger, F.; Hornykiewicz, O. The role of brain edema in epileptic brain damage induced by systemic kainic acid injection. Neuroscience 13:691–704; 1984.
17. McCreery, D.B.; Agnew, W.F. Changes in the extracellular potassium and calcium concentration and neural activity during prolonged electrical stimulation of the cat cerebral cortex at defined charge densities. Exp. Neurol. 79:371–396; 1983.
18. Miyazaki, S.; Ikeda, K. Capacitive electrode for chronic stimulation of nerve. Rep. Inst. Med. Dent. Eng. 63–74; 1974.
19. Olney, J.W.; de Gubareff, T. "Epileptic" brain damage in rats induced by sustained electrical stimulation of the perforant pathway. II. Ultrastructural analysis of acute hippocampal pathology. Brain Res. Bul. 10:699–712; 1983.
20. Olney, J.W.; Fuller, T.A.; de Gubareff, T. Kainate-like neurotoxicity of folates. Nature. 292:165–167; 1981.
21. Petito, C.K.; Pulsinelli, W.A.; Jacobson, G.; Plum, F. Edema and vascular permeability in cerebral ischemia: Comparison between ischemic neuronal damage and infarction. J. Neuropth. Exper. Neurol. 41:423–436; 1982.
22. Pinard, E.; Tremblay, E.; Ben-Ari, Y.; Seylaz, J. Blood flow compensates oxygen demand in the vulnerable CA3 region of the hippocampus during kainate-induced seizures. Neuroscience 13:1039–1049; 1984.
23. Pudenz, R.H.; Agnew, W.F.; Bullara, L.A. Effects of electrical stimulation of the brain. Brain Behavior and Evol. 14:103–135; 1977.
24. Pudenz, R.H.; Bullara, L.A.; Jacques, D.; Hambrecht, F.T. Electrical stimulation of the brain III: The neural damage model. Surg. Neurol. 4:384–400; 1975.
25. Robblee, L.S.; Kelliher, E.M.; Langmuir, M.E.; Vartanian, H.; McHardy, J. Preparation of etched

tantalum semimicro capacitor stimulation electrodes. EIC Laboratories, Inc., Newton, MA. J. Biomed. Mater. Res. (United States). 17:327-343; 1983.
26. Robblee, L.S.; McHardy, J.; Agnew, W.F.; Bullara, L.A. Electrical stimulation with Pt electrodes. VII. Dissolution of Pt electrodes during electrical stimulation of the cat cerebral cortex. J. Neurosci. Meth. 9:301-330; 1983.
27. Rose, T.L.; Kelliher, E.M.; Robblee, L.S. Assessment of capacitor electrodes for intracortical neural stimulation. EIC Laboratories, Inc., Norwood, MA 02062. J. Neurosci. Meth. (Netherlands) 12:181-193; 1985.
28. Schmidt, E.M.; Hambrecht, F.T.; McIntosh, J.S. Intracortical capacitor electrodes: Preliminary evaluation. J. Neurosci. Methods 5:33-39; 1982.
29. Sloviter, R.S.; Damiano, B.P. On the relationship between kainic acid-induced electrophysiological effects and hippocampal damage in rats. Neurosci. Lett. 24:279-284; 1981.
30. Young, R.R.; Cracco, R.Q. Clinical neurophysiology of conduction in central motor pathways. Ann. Neurol. 18:606-610; 1985.
31. Yuen, T.G.H.; Agnew, W.F.; Bullara, L.A.; Jacques, D.; McCreery, D.B. Histological evaluation of neural damage from electrical stimulation: Considerations for the selection of parameters for clinical application. Neurosurg. 9:292-299; 1981.